Coupling analysis in the calibration process of electro-optical detection systems

[1,2]Qijian Tang, [1]Xiangjun Wang, [2]Qingping Yang
[1]MOEMS Education Ministry Key Laboratory, Tianjin University, Tianjin 300072, China
[2]College of Engineering, Design and Physical Sciences, Brunel University London, Uxbridge, UB8 3PH, UK
ytqjtang@163.com, xdocuxjw@vip.163.com, ping.yang@brunel.ac.uk

***Abstract*—Electro-optical detection systems should be calibrated prior to use, a commonly used method with an autocollimator and a high precision turntable may introduce large error in the calibration process. This paper analyzed the calibration process, and showed that the nature of the problem was attributed to the plane rotation around a non-orthogonal axis. The mirror's non-orthogonal rotation was divided into position rotation and mirror spinning, and the effects on autocollimator readout were obtained. Simulation results demonstrated that the coupling effects on elevation and azimuth become serious as the inclined angle and rotated angle increase. It is therefore necessary to separate the coupling error in the calibration process, which would provide more accurate data for further compensation.**

Keywords—coupling analysis; calibration process; rotation; quaternion; EODS

I. INTRODUCTION

Electro-optical detection systems (EODSs) are widely used to collect targets' location information in scientific, military and commercial applications, they can be installed on vehicles, ships, aircrafts and spacecraft [1-2]. In some important applications, the pointing accuracy of line of sight (LOS) is vital to EODS in case of precise location, however, it is often affected by various error sources such as axial misalignments, nonperpendicularity, etc. It is thus necessary to determine and compensate for the pointing errors [3]. Autocollimator and turntable are often utilized to calibrate EODS. Sometimes, a laser tracker could also be used to measure the rotated angle of EODS without turntable. As shown in Fig.1, a two axial EODS is placed on a high precision turntable, a plane mirror is fixed on the inner gimbal of the EODS. The high precision turntable is used to provide reference angle of rotation, EODS will rotate the same angle in the opposite direction, and the bias will be presented by the autocollimator readouts. Assume the autocollimator readout is zero at initial position where respective azimuth axes are perpendicular to the vertical direction, and elevation axes are parallel to the vertical direction, then the turntable rotates θ_{TA} and θ_{TE} around its azimuth axis and elevation axis, respectively. The EODS rotates $\theta_{PA}$and θ_{PE} around its azimuth axis and elevation axis. We define the autocollimator readouts are respective ΔA and ΔE in horizontal and vertical directions. Ideally, there should be:

$$\begin{cases}\Delta A = -\theta_{TA} + \theta_{PA} \\ \Delta E = -\theta_{TE} + \theta_{PE}\end{cases} \quad (1)$$

But it can be shown there are significant errors in the above angle relationships, which is the main problem to be discussed in this paper.

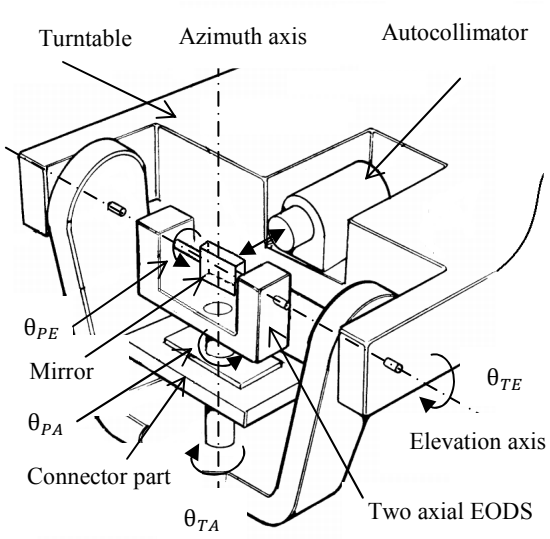

Fig. 1. Calibration system of EODS

II. ERROR SAUCE ANALYSIS

In Fig.1, if $\theta_{PE} = 0$ and $\theta_{TE} = 0$, it is easy to obtain $\Delta A = -\theta_{TA} + \theta_{PA}$, similarly, if $\theta_{PA} = 0$ and $\theta_{TA} = 0$, then $\Delta E = -\theta_{TE} + \theta_{PE}$. In this case, the rotation axis is perpendicular to the normal axis of plane mirror, we define the rotation as 'mirror rotation'. In case of $\theta_{PE} \neq 0$ and $\theta_{TE} \neq 0$, if $\Delta E = 0$, the incident light from autocollimator is still perpendicular to the plane mirror, we define $\Delta\theta_A = -\theta_{TA} + \theta_{PA}$, then the mirror will rotates $\Delta\theta_A$ around a non-orthogonal axis which has an inclined angle θ_{PE} with the vertical axis. In the worst case, $\theta_{PE} = 90°$, the mirror rotates around its normal axis, which would have no effect on the autocollimator readouts. In this case, we define the rotation as 'mirror spinning'. If $0 < |\theta_{PE}| < 90°$, it is apparent that the rotation around the azimuth axis of the EODS can be divided into mirror rotation and mirror spinning. As a result, the readouts from the autocollimator will couple between azimuth and elevation biases.

The work was supported by Support Program of National Ministry of Education of China (No.625010110) and National Natural Science Foundation of China (No.61179043). It was also supported by China Scholarship Council.

III. ROTATION DECOMPOSITION

The mirror rotation is attributed to plane rotation around a non-orthogonal axis. As shown in Fig. 2, plane Ω_1 rotates 2θ ($0° \leq |2\theta| \leq 90°$) around OP to Ω_2, the projection of OP in Ω_1 is the vertical axis, and their inclined angle is α. If Ω_1 rotates around the vertical axis, the reflected light spot will move in the horizontal direction. If it rotates around OP, the light spot will deviate from the horizontal direction.

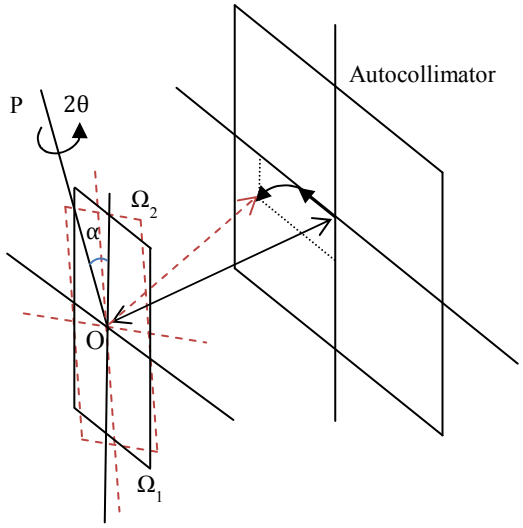

Fig. 2. Plane rotation diagram

As demonstrated in Fig. 3, plane $OPC_1 \perp \Omega_1$, plane $OPC_2 \perp \Omega_2$, $\overrightarrow{OD_1}$, $\overrightarrow{OD_2}$ and $\overrightarrow{OD_3}$ are normal vectors of Ω_1, Ω_2, and plane C_1OC_2, respectively. $\overrightarrow{QC_1} \perp \overrightarrow{OQ}$, $\overrightarrow{QC_2} \perp \overrightarrow{OQ}$, $\overrightarrow{PC_1} \perp \overrightarrow{OC_1}$, $\overrightarrow{PC_2} \perp \overrightarrow{OC_2}$, $\angle C_1QC_2 = 2\theta$, $\angle POC_1 = \angle POC_2 = \alpha$. It is apparent that the inclined angle between Ω_1 and plane C_1OC_2 is the same as that between plane C_1OC_2 and Ω_2, which we define as δ, it is also the inclined angle between $\overrightarrow{OD_1}$ and $\overrightarrow{OD_3}$. Let $\angle C_1OC_2 = 2\gamma$, then the rotation process can be decomposed into three steps:

- Ω_1 rotates δ around OC_1 to plane C_1OC_2;
- Plane C_1OC_2 spins 2γ around OD_3;
- Plane C_1OC_2 rotates δ around OC_2 to Ω_2.

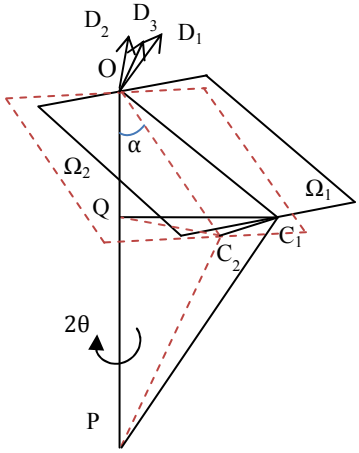

Fig. 3. Plane rotation decomposition

We define plane POC_1 as the plane XOZ, OP as the OZ, and establish the coordinate system as shown in Fig. 4. Quaternions represented by just four scalars can be used to speed up calculations involving rotations, in contrast to a 3×3 rotation matrix which has nine scalar entries [4-6].

A quaternion is defined as follows, and the detailed information is presented in reference [5].

$$Q = a\boldsymbol{i} + b\boldsymbol{j} + c\boldsymbol{k} + q_0 \tag{2}$$

where a, b, c and q_0 are the real numbers, and $\boldsymbol{i}, \boldsymbol{j}$ and $\boldsymbol{k}$ are the imaginary units which obey the following multiplication rules:

$$\begin{cases} \boldsymbol{i}^2 = \boldsymbol{j}^2 = \boldsymbol{k}^2 = -1 \\ \boldsymbol{ij} = -\boldsymbol{ji} = \boldsymbol{k} \\ \boldsymbol{ki} = -\boldsymbol{ik} = \boldsymbol{j} \\ \boldsymbol{jk} = -\boldsymbol{kj} = \boldsymbol{i} \end{cases} \tag{3}$$

Let $\boldsymbol{q} = a\boldsymbol{i} + b\boldsymbol{j} + c\boldsymbol{k}$, equation (2) can be rewritten as:

$$Q = q_0 + \boldsymbol{q} \tag{4}$$

where q_0 denotes the scalar part, and q denotes the vector part.

A vector $\mathbf{R_s}$ rotates 2θ around $\mathbf{n}$ ($\mathbf{n}$ is the unit vector) to $\mathbf{R_s}'$, and the resulting vector can be computed through rotation transformation as shown in (5).

$$\mathbf{R_s}' = Q\mathbf{R_s}Q^* \tag{5}$$

where Q is the rotation quaternion, and $Q = \cos\theta + \mathbf{n}\sin\theta$, $Q^* = \cos\theta - \mathbf{n}\sin\theta$ is the conjugate of Q.

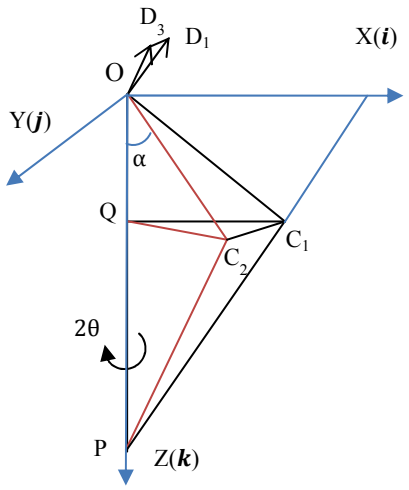

Fig. 4. Angle solving diagram

From Fig. 4, $\overrightarrow{OC_1}$rotates 2θ around $\overrightarrow{OP}$ to $\overrightarrow{OC_2}$, thus it has:

$$\overrightarrow{OC_2} = Q_{oz}\overrightarrow{OC_1}{Q_{oz}}^* \tag{6}$$

where $Q_{oz} = \cos\theta + \boldsymbol{k}\sin\theta$. As $\overrightarrow{OD_1}$ and $\overrightarrow{OD_3}$ are normal vectors of $\Omega_1$and plane C_1OC_2, then it has:

$$\begin{cases} \overrightarrow{OD_1} \perp \overrightarrow{OC_1}, \overrightarrow{OD_1} \in \text{plane XOZ} \\ \overrightarrow{OD_3} \perp \overrightarrow{OC_1}, \overrightarrow{OD_3} \perp \overrightarrow{OC_2} \end{cases} \tag{7}$$

Combined (6) and (7), it can be obtained:

$$\begin{cases} 2\delta = 2\sin^{-1}\left(\frac{\sin\theta\cos\alpha}{\sqrt{1-\sin^2\theta\sin^2\alpha}}\right) \\ 2\gamma = 2\sin^{-1}(\sin\theta\sin\alpha) \end{cases} \tag{8}$$

IV. Readouts Coupling Analysis

Based on the three steps' decomposition above, in the first step, the mirror rotates δ around the vertical axis, then the autocollimator readouts in horizontal and vertical directions are respective ΔA_1 and ΔE_1:

$$\begin{cases} \Delta A_1 = \delta \\ \Delta E_1 = 0 \end{cases} \tag{9}$$

In the second step, the mirror spins 2γ around $\overrightarrow{OD_3}$, the autocollimator readouts both in horizontal and vertical directions remain the same. In the third step, the mirror rotates δ around $\overrightarrow{OC_2}$, not the vertical axis, and the readouts in two directions are given in (10):

$$\begin{cases} \Delta A_2 = \frac{1}{2}\tan^{-1}(\tan 2\delta\cos 2\gamma) \\ \Delta E_2 = \frac{1}{2}\tan^{-1}(\tan 2\delta\sin 2\gamma) \end{cases} \tag{10}$$

In hence, the effect of the non-orthogonal rotation of azimuth is given in (11):

$$\begin{cases} \Delta A = \Delta A_1 + \Delta A_2 = \delta + \frac{1}{2}\tan^{-1}(\tan 2\delta\cos 2\gamma) \\ \Delta E = \Delta E_1 + \Delta E_2 = \frac{1}{2}\tan^{-1}(\tan 2\delta\sin 2\gamma) \end{cases} \tag{11}$$

If there is a tiny deviation of $\Delta\theta_E$ before azimuth rotation, it will not affect azimuth readout, and the elevation readout can be rewritten as:

$$\Delta E = \Delta E_1 + \Delta E_2 + \Delta E_0 = \frac{1}{2}\tan^{-1}(\tan 2\delta\sin 2\gamma) + \Delta\theta_E \tag{12}$$

V. Simulation Results

Assume the rotated angle 2θ of EODS is -20°~20°, the inclined angle α is -60°~60°. Combined with Fig.1, it means $\Delta\theta_A = (-\theta_{TA} + \theta_{PA}) = 2\theta \in [-20°, 20°]$ and $\theta_{TE} = \theta_{PE} = \alpha \in [-60°, 60°]$. Ideally, the autocollimator readouts satisfy:

$$\begin{cases} \Delta A = -\theta_{TA} + \theta_{PA} \\ \Delta E = 0 \end{cases} \tag{13}$$

However, according to equation (11), the effects on azimuth and elevation readouts are different from (13). As presented in Fig. 5, the azimuth readout of autocollimator changes as the rotated angle and inclined angle increase. At the same time, elevation readouts are no longer zero. And the coupling effect on elevation is presented on the right in Fig. 5. Fig. 6 denotes the bias between ideal azimuth readout of the autocollimator and simulated readout, which indicate that the rotation effect for the azimuth becomes serious as θ and α increase. In the worst case, if $\alpha = 90°$, the simulated readout is zero, it only has mirror spinning. In addition, it should be noted that if $\Delta\theta_A$ is minute, which means 2θ is minute, equations (11) and (12) can be simplified as:

$$\begin{cases} \Delta A = \Delta\theta_A\cos\alpha \\ \Delta E = \Delta\theta_E \end{cases} \tag{14}$$

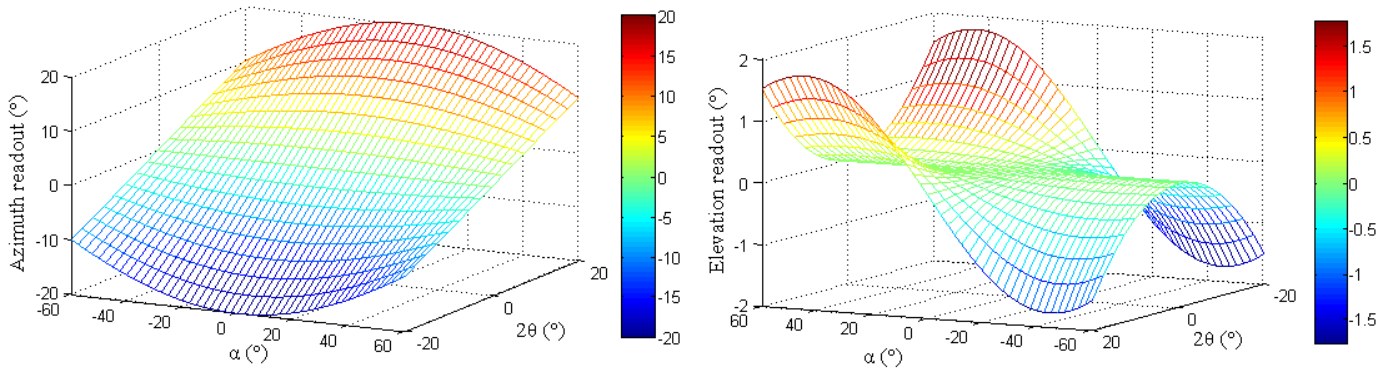

Fig. 5. Non-orthogonal rotation effects on both azimuth and elevation

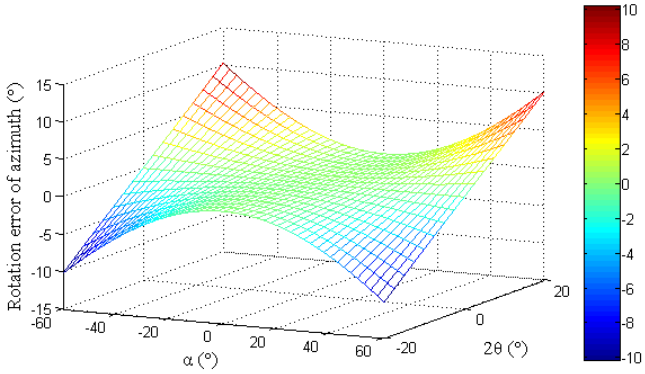

Fig. 6. Rotation error of azimuth

VI. CONCLUSIONS

Concerning the commonly used calibration method with an autocollimator and a high precision turntable for EODS, this paper established a mathematical model about the coupling problem in the rotation process. The rotation process which introduced rotation deviation and coupling problem was decomposed into three steps, and the effects on azimuth and elevation were obtained by means of quaternions. The simulation results demonstrated that the calibration method would introduce significant error in pointing accuracy in case of large inclined angle and azimuth bias. With the relevant equations obtained in this paper, the rotation effects could be effectively separated, which would provide more accurate data for further compensation.

REFERENCES

[1] J. Hilkert, "Inertially stabilized platform technology," IEEE Contr. Syst. Mag. vol. 28, pp.26–46, 2008.

[2] K. Michael, "Inertially stabilized platforms for optical imaging systems," IEEE Contr. Syst. Mag. vol.28, pp.47–64, 2008.

[3] A. Rue, "Calibration of precision gimballed pointing systems," IEEE Trans. Aero. Elec. Syst. vol.AES-6, pp.697-706, 1970.

[4] R. Goldman, "Understanding quaternions," Graph. Models. vol.73, pp.21-49, 2011.

[5] L. Meister and H. Schaeben, "A concise quaternion geometry of rotations," Math. Meth. Appl. Sci. vol.28, pp.101-126, 2005.

[6] L. Meister, "Mathematical modelling in geodesy based on quaternion algebra," Phys. Chem. Earth (A). vol.25, pp.661-665, 2000.